



SiOxNy:B layers for ex-situ doping of hole-selective poly silicon contacts: A passivation study

Audrey Morisset, Raphaël Cabal, Valentin Giglia, Bernadette Grange, J Alvarez, Marie-Estelle Gueunier-Farret, Sébastien Dubois, Jean-Paul Kleider

► To cite this version:

Audrey Morisset, Raphaël Cabal, Valentin Giglia, Bernadette Grange, J Alvarez, et al.. SiOxNy:B layers for ex-situ doping of hole-selective poly silicon contacts: A passivation study. SiliconPV 2019, THE 9TH INTERNATIONAL CONFERENCE ON CRYSTALLINE SILICON PHOTOVOLTAICS, Apr 2019, Leuven, Belgium. pp.040012, 10.1063/1.5123839 . hal-02330432

HAL Id: hal-02330432

<https://hal.archives-ouvertes.fr/hal-02330432>

Submitted on 11 Mar 2020

HAL is a multi-disciplinary open access archive for the deposit and dissemination of scientific research documents, whether they are published or not. The documents may come from teaching and research institutions in France or abroad, or from public or private research centers.

L'archive ouverte pluridisciplinaire **HAL**, est destinée au dépôt et à la diffusion de documents scientifiques de niveau recherche, publiés ou non, émanant des établissements d'enseignement et de recherche français ou étrangers, des laboratoires publics ou privés.

SiOxNy:B layers for ex-situ doping of hole-selective poly silicon contacts: A passivation study

Cite as: AIP Conference Proceedings **2147**, 040012 (2019); <https://doi.org/10.1063/1.5123839>
Published Online: 27 August 2019

Audrey Morisset, Raphaël Cabal, Valentin Giglia, Bernadette Grange, José Alvarez, Marie-Estelle Gueunier-Farret, Sébastien Dubois, and Jean-Paul Kleider



View Online



Export Citation

AIP | Conference Proceedings

Get **30% off** all
print proceedings!

Enter Promotion Code **PDF30** at checkout



SiO_xN_y:B Layers for Ex-situ Doping of Hole-Selective Poly Silicon Contacts: A Passivation Study

Audrey Morisset^{1,2,3 a)}, Raphaël Cabal^{1,b)}, Valentin Giglia¹, Bernadette Grange¹,
José Alvarez^{2,3}, Marie-Estelle Gueunier-Farret^{2,3}, Sébastien Dubois¹,
Jean-Paul Kleider^{2,3}

¹Univ. Grenoble Alpes, INES, F-73375 Le Bourget du Lac, France ; CEA, LITEN, Département des Technologies Solaires, F-73375 Le Bourget du Lac, France

²Laboratoire de Génie Electrique et Electronique de Paris, CNRS UMR 8507, SUPELEC, Univ. Paris-Sud, Sorbonne Universités-UPMC Univ. Paris 06, F-91192 Gif-sur-Yvette Cedex, France

³Institut Photovoltaïque d'Ile-de-France (IPVF), 91120 Palaiseau, France

^{a)}Corresponding author: audrey.morisset@cea.fr

^{b)}raphael.cabal@cea.fr

Abstract. Passivating the contacts of crystalline silicon (c-Si) solar cells with a polycrystalline silicon layer (poly-Si) on a thin oxide (SiO_x) film allows to decrease the recombination current at the metal/c-Si interface. In this study, an ex-situ doping method of poly-Si is proposed, involving a SiO_xN_y:B layer as a dopant source. In this study, we compare the properties (crystallinity of the deposited layer, doping profile and surface passivation properties) of the resulting ex-situ doped poly-Si(B) layer with our in-situ doped reference.

INTRODUCTION

Passivating the contacts of c-Si solar cells with a polycrystalline silicon (poly-Si) layer on top of a thin silicon oxide (SiO_x) is known to reduce carrier recombination at the interface between the metal electrodes and the c-Si substrate¹⁻³. In this study we focused on boron-doped poly-Si (poly-Si(B)) structures which are of prime interest to passivate the rear side of next-generation PERC solar cells. Poly-Si(B) layers are prepared by Plasma-Enhanced Chemical Vapor Deposition (PECVD) of an amorphous silicon (a-Si:H) layer followed by a crystallization annealing step. Poly-Si(B) layers were previously developed in our lab by in-situ doping the a-Si:H layer with the addition of B₂H₆ to the precursor gas mix⁴. However, the use of H-rich precursor gases during the PECVD step is leading to a blistering phenomenon of the layer^{5,6}. Moreover, the addition of B to the deposited layer is impeding the crystallization of the in-situ doped poly-Si(B) layer⁷.

For these reasons we developed an ex-situ doping method which consists in depositing a B-rich dielectric layer (SiO_xN_y:B) on top of an intrinsic Si layer deposited by PECVD. In this contribution we compared the ex-situ doped poly-Si(B) layer with our reference in-situ doped poly-Si(B): we first studied the effect of removing the B₂H₆ during the PECVD step on the crystalline nature of the deposited layer. Then, we confront the active doping profiles of poly-Si(B) layers obtained with in-situ and ex-situ doping methods. Finally, we compare the passivation properties of in-situ and ex-situ doped poly-Si(B)/SiO_x structures as function of the annealing temperature.

EXPERIMENTAL

Symmetrical samples were prepared from 180 μm-thick KOH-polished 156 mm n-type Cz wafers (3-6 Ω.cm). First, a thin SiO_x layer (~1.3 nm) was grown on the surface of the wafers by ozonized DI-H₂O rinsing. Reference

in-situ doped poly-Si(B) layers were prepared by PECVD of 25 nm-thick B-doped a-Si:H layers on both sides of the wafer using H₂-diluted diborane (B₂H₆) as doping precursor gas and followed by an annealing step under argon (T_a = 700-900°C) to crystallize the layer and activate dopants. Ex-situ doped poly-Si(B) layers were prepared by PECVD of a SiO_xN_y:B layer on top of a 25 nm-thick intrinsic Si layer deposited by PECVD, followed by the same annealing step to ensure dopant diffusion and activation. A hydrogenation step was carried out on both in-situ and ex-situ poly-Si(B) layers by PECVD of a H-rich silicon nitride (SiN:H) layer, followed by a firing step in a belt furnace (T_{firing} = 800-900°C).

Thicknesses of initial a-Si and final poly-Si layers were measured by spectroscopic ellipsometry (SE) respectively after PECVD and crystallization annealing. The imaginary part of the dielectric function (ϵ_i) obtained as a function of the photon energy (E_p) through SE measurement was used to assess the crystalline nature of the layers. Electrochemical Capacitance-Voltage (ECV) and Hall effect measurements were performed to respectively assess the active doping profile and electrical properties (carrier density, conductivity and mobility) of the final poly-Si(B) layers. Eventually, the photo-conductance decay (PCD) technique was used to evaluate the surface passivation properties (in terms of implied open circuit voltage (iV_{oc}) and recombination current density (J_0)) of in-situ and ex-situ doped poly-Si(B)/SiO_x structures.

RESULTS AND DISCUSSION

Effect of B₂H₆ Removal on the Deposited Layer

In this paragraph, we compare the crystalline nature of the B-doped and intrinsic Si layer after deposition.

In-situ B-doped a-Si:H layer were previously developed in our lab by PECVD. The use of a high deposition temperature (T_{dep} = 300°C) and a high gas ratio (R = H₂/SiH₄ = 50) afforded blister-free passivating poly-Si(B)/SiO_x structures after annealing⁴. The use of a high gas ratio R during PECVD could promote a deposition of microcrystalline Si layers (μ c-Si)⁸. However, the addition of B during the process is known to impede its crystallization⁷. Indeed, our B-doped layer was verified to be amorphous after deposition as the curve representing ϵ_i versus E_p featured a broad peak centered around 3.3 eV (for a layer thickness of 25 nm, see Fig. 1)⁹. Therefore we denote the in-situ B-doped layer after deposition as: a-Si:H(B).

In order to use an ex-situ doping method we needed to develop an intrinsic layer by PECVD. For this purpose we used the same PECVD parameters than the ones used for a-Si:H(B) deposition except that we removed B₂H₆ from the precursor gases. This resulted in the crystallization of the deposited layer into a μ c-Si intrinsic layer (μ c-Si(i)). The μ c nature of the layer was evidenced by SE as the ϵ_i versus E_p curve featured a plateau shape due to the apparition of a second peak around 4.1 eV typical of a μ c-Si phase⁹ (see Fig. 1).

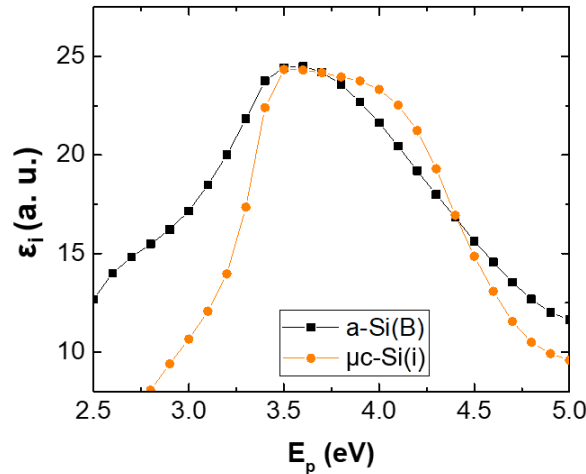


FIGURE 1. Imaginary part of the dielectric function (ϵ_i) vs. photon energy (E_p), from SE measurement performed after deposition of in-situ doped a-Si:H(B) layer and intrinsic μ c-Si(i) (both 25 nm-thick). The removal of the doping precursor gas B₂H₆ had the effect of changing the nature of the deposited layer from amorphous to microcrystalline (a-Si to μ c-Si).

In-situ and Ex-situ Poly-Si(B) Doping Profiles

In this paragraph we compare the active-doping profiles obtained on reference in-situ doped poly-Si(B) layers and on ex-situ doped poly-Si(B) layers. The active-doping profiles were measured by ECV after annealing in the range $T_a = 700\text{-}800^\circ\text{C}$ (Fig. 2). For $T_a = 700\text{-}750^\circ\text{C}$, a gradually fading doping density was observed for the ex-situ doped layer (from $2 \times 10^{19} \text{ cm}^{-3}$ to $2 \times 10^{18} \text{ cm}^{-3}$). In this T_a range, the in-situ doping profile showed more of a plateau around $1.5 \times 10^{20} \text{ cm}^{-3}$. For $T_a = 800^\circ\text{C}$, although the shape of the in-situ and ex-situ doping profiles were similar, the doping density in the ex-situ layer was found to be ten times lower than the doping density in the in-situ layer. Interestingly, for $T_a = 800^\circ\text{C}$, the B-diffusion length in the c-Si was found to be similar for both in-situ and ex-situ doped layers. For $T_a = 850^\circ\text{C}$ (not shown here), the doping plateau remained similar as for $T_a = 800^\circ\text{C}$ for both in-situ and ex-situ poly-Si layers but the B-diffusion tail into c-Si was deeper (respectively 150 nm and 100 nm-deep for in-situ and ex-situ layers).

Hall effect measurements were performed on in-situ and ex-situ doped layers for $T_a = 700^\circ\text{C}$ to avoid any B-diffusion in the c-Si that could induce current flowing in the c-Si and therefore would not enable an accurate estimation of the poly-Si electrical properties. The ex-situ carrier density measured was lower than the in-situ one ($1.2 \times 10^{19} \text{ cm}^{-3}$ and $1 \times 10^{20} \text{ cm}^{-3}$ respectively), which is consistent with the ECV doping profiles showing a lower doping density for the ex-situ doped layer.

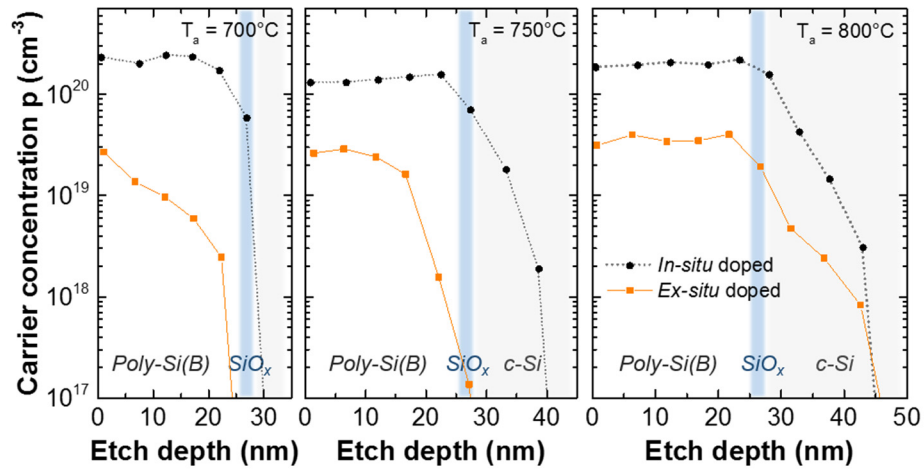


FIGURE 2. ECV active doping profiles of in-situ and ex-situ doped poly-Si(B) layers (25 nm-thick) after annealing at T_a . The SiO_x layer is depicted for reference.

Surface Passivation Properties

The passivation level provided by the ex-situ doped poly-Si(B) structure was then evaluated (in terms of iV_{oc} and J_0) as a function of the annealing temperature (T_a), after annealing and after SiN:H deposition (i.e. before firing). It was compared to the passivation level obtained with in-situ doped poly-Si layer (see Fig. 3). It is to note that the stability of the bulk effective carrier lifetime was verified on the range of T_a investigated.

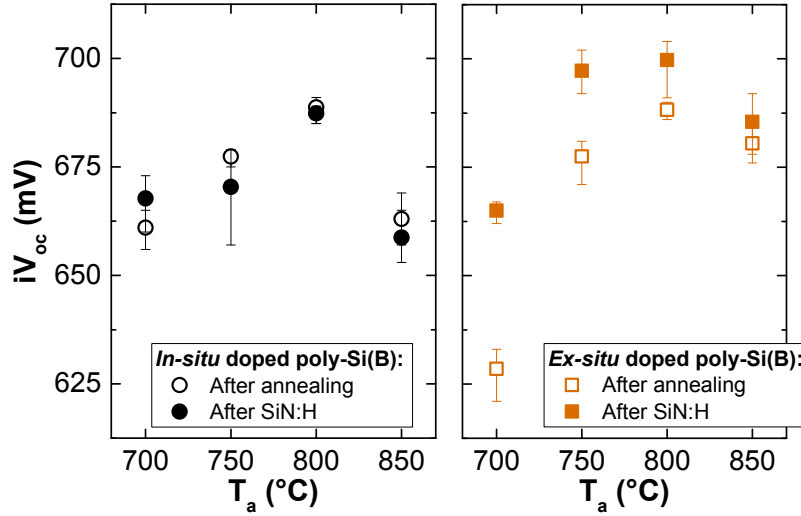


FIGURE 3. iV_{oc} as function of T_a with in-situ and ex-situ doped poly-Si/SiO_x after annealing and right after SiN:H deposition (before firing).

After annealing, the iV_{oc} evaluated on in-situ and ex-situ structures showed a similar trend featuring an increase of the iV_{oc} value from 700°C to 800°C and a decrease of iV_{oc} for $T_a > 800^\circ\text{C}$. For T_a in the range 750°C – 850°C, the iV_{oc} values measured with both structures were equivalent. For $T_a = 700^\circ\text{C}$, the ex-situ doped structure showed lower passivation properties than the in-situ doped structure (iV_{oc} of 628.5 mV and 661 mV respectively). This could be the result of a lower field-effect passivation provided by the ex-situ poly-Si layer that was only partially doped for $T_a = 700^\circ\text{C}$ (see Fig. 2). The subsequent SiN:H deposition involved only slight changes in the iV_{oc} measured on in-situ doped structures whereas it enabled an iV_{oc} gain for ex-situ doped structures on all the T_a range investigated (up to 30 mV for $T_a = 700^\circ\text{C}$). This resulted in slightly higher passivation level provided by the ex-situ doped poly-Si/SiO_x structure after SiN:H deposition, with a maximum iV_{oc} of 702 mV. For both in-situ and ex-situ layers, the drop of iV_{oc} for $T_a > 800^\circ\text{C}$ was attributed to the degradation of the SiO_x layer¹⁰ and/or excessive B-diffusion in the c-Si¹¹.

After subsequent firing at $T_f \sim 860^\circ\text{C}$, an important gain in surface passivation was observed for both in-situ and ex-situ doped poly-Si/SiO_x structures on all the T_a range investigated. Best iV_{oc} values of 736 mV for in-situ structures and 733 mV for ex-situ structures were obtained after annealing at $T_a = 750^\circ\text{C}$ (both corresponding to $J_0 = 6 \text{ fA}\cdot\text{cm}^{-2}$). In conclusion, despite the lower doping density of the ex-situ poly-Si layer, the final passivation properties offered by in-situ and ex-situ poly-Si/SiO_x structures were found to be equivalent.

CONCLUSION

We proposed an ex-situ doping method for poly-Si passivating structures using a boron-rich dielectric layer as a dopant source and we compared the properties of the resulting ex-situ doped poly-Si layer to our reference in-situ doped layer. First, we observed that the removal of the B-rich doping gas during PECVD resulted in crystallization of the deposited layer. Then, the active doping profiles of in-situ and ex-situ poly-Si layers were compared. The doping density of the ex-situ poly-Si layer was observed to be ten times lower than the in-situ layer. Finally, we evaluated the surface passivation provided by in-situ and ex-situ doped poly-Si/SiO_x structures after different step of the process. After annealing both structures showed equivalent surface passivation properties. After SiN:H deposition and subsequent firing, both in-situ and ex-situ structures showed excellent surface passivation. Best $\{iV_{oc}; J_0\}$ couple were of $\{736 \text{ mV}; 6 \text{ fA}\cdot\text{cm}^{-2}\}$ and $\{733 \text{ mV}; 6 \text{ fA}\cdot\text{cm}^{-2}\}$ for in-situ and ex-situ structures respectively.

ACKNOWLEDGMENTS

The team gratefully acknowledge the IPVF (Institut Photovoltaïque d’Ile de France) for financial support. This project received funding from French National Research Agency (Programs “Investment for the Future” ANR-IEED-002-01, ANR-10-ITE-0003 and “Oxygen” ANR-17-CE05-0035).

REFERENCES

1. A. Richter, J. Benick, F. Feldmann, A. Fell, M. Hermle, and S.W. Glunz, *Sol. Energy Mater. Sol. Cells* **173**, 96 (2017).
2. F. Haase, C. Hollemann, S. Schäfer, A. Merkle, M. Rienäcker, J. Krügener, R. Brendel, and R. Peibst, *Sol. Energy Mater. Sol. Cells* **186**, 184 (2018).
3. G. Nogay, A. Ingenito, E. Rucavado, Q. Jeangros, J. Stuckelberger, P. Wyss, M. Morales-Masis, F.-J. Haug, P. Loper, and C. Ballif, *IEEE J. Photovolt.* **1** (2018).
4. A. Morisset, R. Cabal, B. Grange, C. Marchat, J. Alvarez, M.-E. Gueunier-Farret, S. Dubois, and J.-P. Kleider, *Phys. Status Solidi A* **1800603** (2018).
5. B. Nemeth, D.L. Young, M.R. Page, V. LaSalvia, S. Johnston, R. Reedy, and P. Stradins, *J. Mater. Res.* **31**, 671 (2016).
6. Y. Tao, E.L. Chang, A. Upadhyaya, B. Roundaville, Y.-W. Ok, K. Madani, C.-W. Chen, K. Tate, V. Upadhyaya, and F. Zimbardi, in *Photovolt. Spec. Conf. PVSC 2015 IEEE 42nd* (IEEE, 2015), pp. 1–5.
7. C. Voz, D. Peiro, J. Bertomeu, D. Soler, M. Fonrodona, and J. Andreu, *Mater. Sci. Eng. B* **69–70**, 278 (2000).
8. J. Koh, Y. Lee, H. Fujiwara, C.R. Wronski, and R.W. Collins, *Appl. Phys. Lett.* **73**, 1526 (1998).
9. G.E. Jellison, M.F. Chisholm, and S.M. Gorbalkin, *Appl. Phys. Lett.* **62**, 3348 (1993).
10. G.R. Wolstenholme, N. Jorgensen, P. Ashburn, and G.R. Booker, *J. Appl. Phys.* **61**, 225 (1987).
11. F. Feldmann, J. Schoen, J. Polzin, J. Niess, W. Lerch, M. Hermle, 9th International Conference on Crystalline Photovoltaics (SiliconPV), Leuven, Belgium, 2019.